

Detection of common bunt disease in wheat kernels and ears using visible and near-infrared hyperspectral imaging

C. DEMOITIE¹, D. VINCKE¹, D. EYLENBOSCH², W. R. MEZA MORALES², C. BATAILLE³ and P. VERMEULEN¹

¹Quality and authentication of agricultural products Unit, ²Crop production Unit and ³Crop and forest health Unit
Wallon Agricultural Research Centre (CRA-W), Gembloux, Belgium

Contact: c.demoitie@cra.wallonie.be

Common wheat bunt disease

Common wheat bunt is a highly pathogenic fungal disease (mainly caused by *Tilletia caries* in Wallonia, Belgium) that affects crops yield and quality. Infected ears are characterized by a ruffled appearance revealing at maturity short, dark and rounded kernels (cf. figure 1). Bunt-affected kernels are filled with millions of spores which are easily released during harvesting and storage, and can thus contaminate the soil and surrounding healthy kernels.

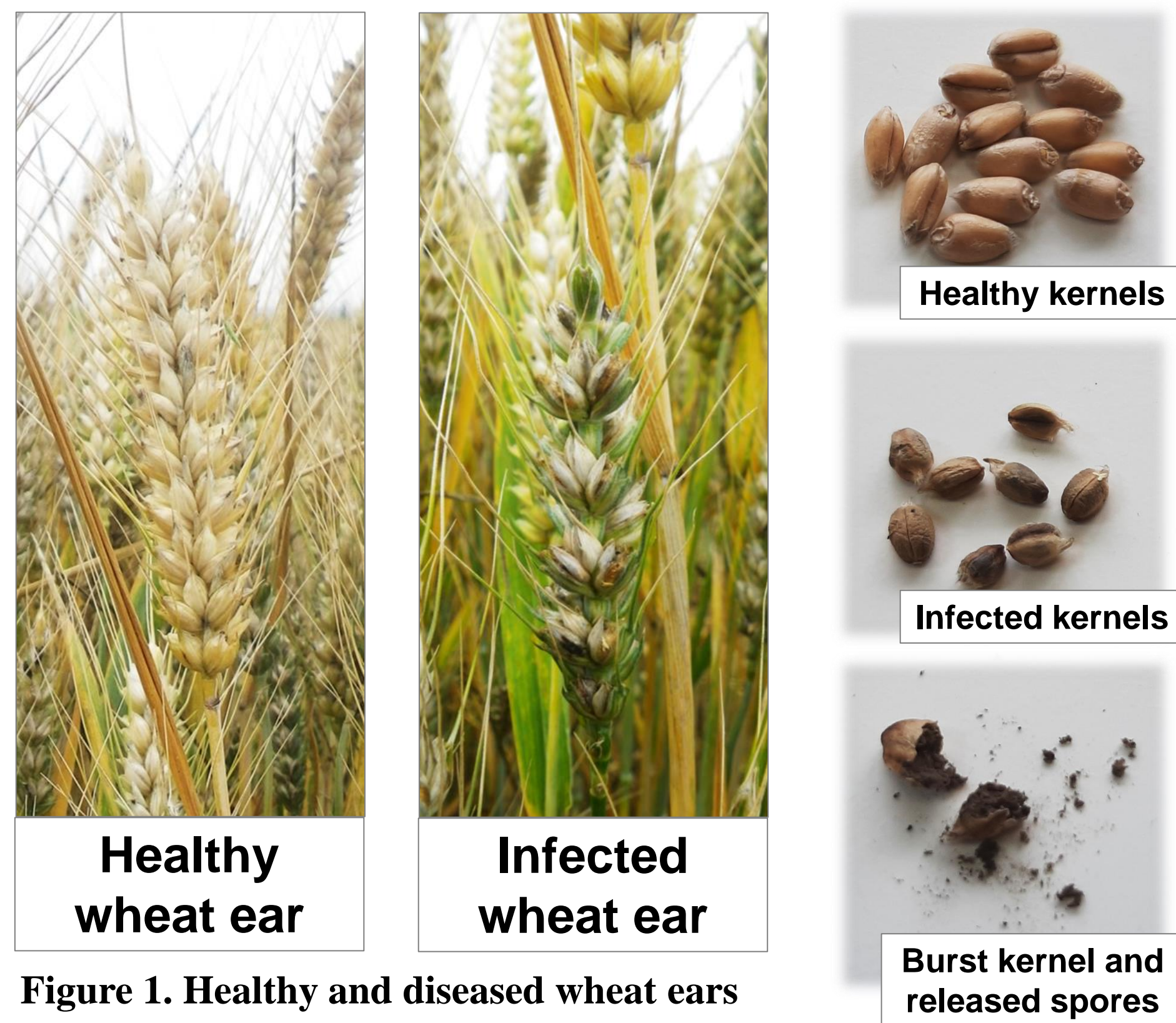


Figure 1. Healthy and diseased wheat ears and kernels.

Diseased kernels detection

Near-infrared hyperspectral imaging (NIR HSI) has already shown its potential to detect impurities and contaminants such as ergot bodies in cereal batches. Kernels measurements were taken on the linescan hyperspectral camera SWIR XEVA (SPECIM, Finland) working in the spectral range from 1100 to 2400 nm and coupled with a conveyor belt (BurgerMetrics, Latvia). Bunt spores exhibit a spectral profile showing a high lipid content allowing a discrimination from healthy kernels in the spectral range between 2300 and 2400 nm (cf. figure 2). A dichotomous classification tree based on five partial least square discriminant analysis (PLS-DA) models was used to detect successively healthy kernels, whole infected kernels, burst infected kernels, clusters of spores and wheat impurities (straw or husk) in a sample (cf. figure 3).

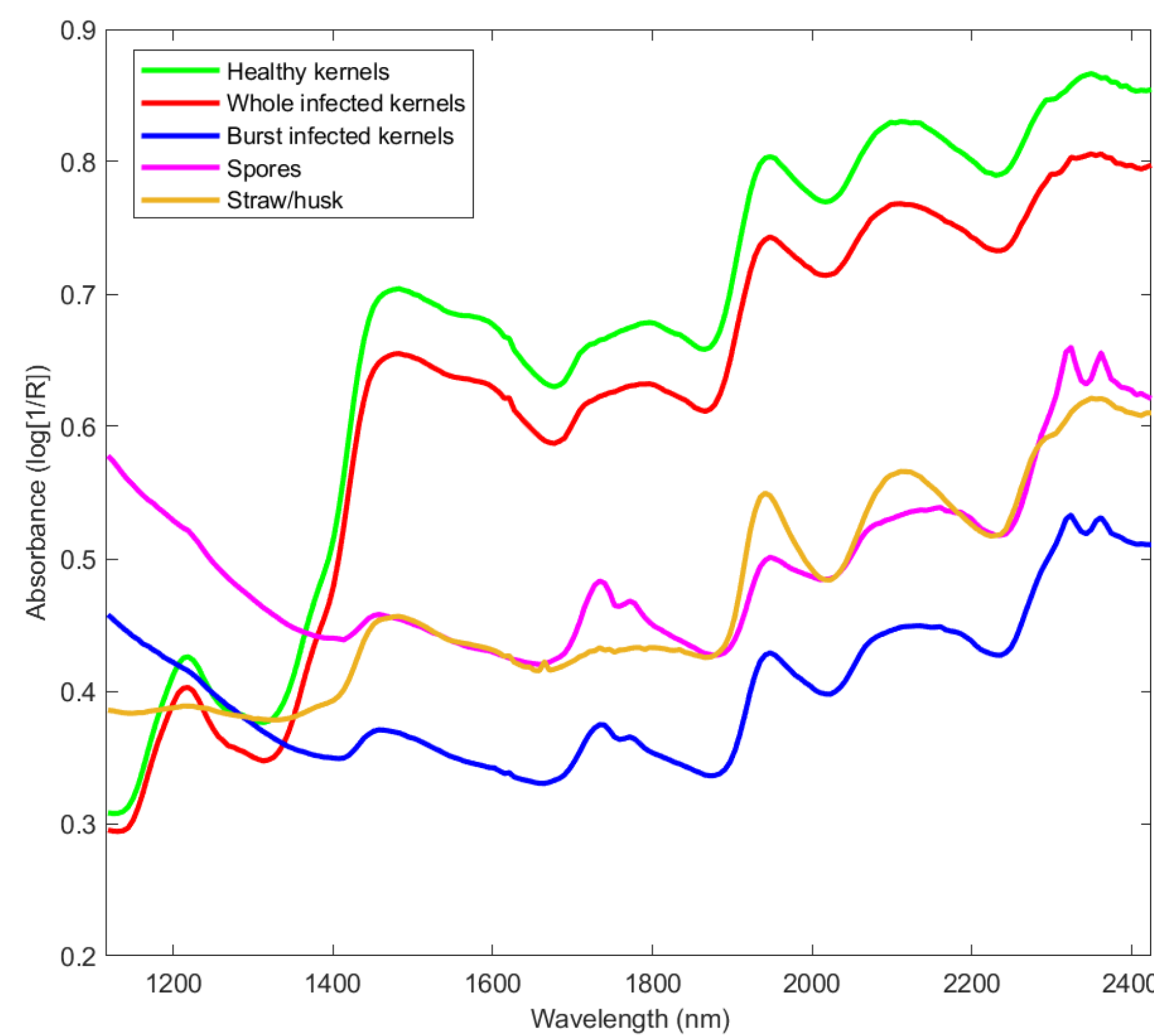


Figure 2. Mean spectra of the SWIR XEVA discriminated classes.

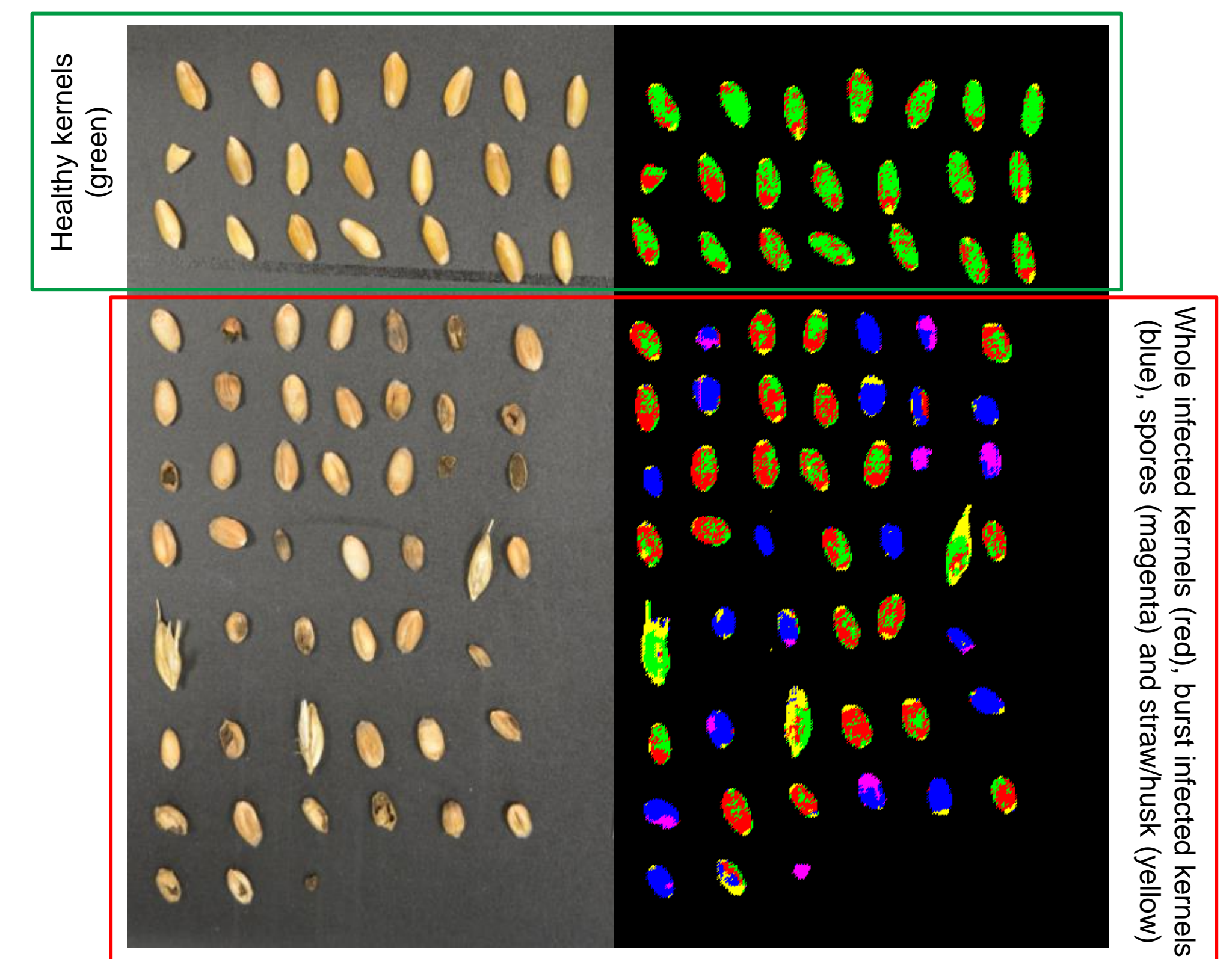


Figure 3. Prediction image of the models developed on SWIR XEVA in validation.

Diseased ears detection

Wheat ear samples were collected before harvest from bunt inoculated test plots in 2022 and 2023; they were then stored in micro-perforated plastic bags after the visual assessment of the health status. Individual ears were measured with the linescan hyperspectral cameras FX10 [400-1000 nm] and FX17 [900-1700 nm] (SPECIM, Finland) combined with a sample tray (21 cm × 40 cm) mounted on a motorized linear translation stage (Labscanner, SPECIM, Finland). Two image analysis approaches were investigated for discrimination:

- one PLS-DA model per camera based on the mean spectra of each ear to discriminate between healthy and diseased ears (cf. table 1);
- three PLS-DA models per camera applied successively at pixel-level to discriminate the different parts of the ears, namely the awns, leaves and stem, and the parts containing healthy and infected kernels (cf. table 2 and figure 4).

1. Discrimination based on the mean spectra of each ear

Calibration set: 30 ears from 2 varieties (19 healthy and 11 with bunt disease)
Validation set: 246 ears from 15 varieties (130 healthy and 116 with bunt disease)
Significant wavelengths: FX10: at 690 nm, between 900 and 1000 nm
 FX17: between 1160 and 1200 nm, 1400 nm
 → Areas attributable to the presence of water and starch¹.

Table 1. Performances in validation of the classification models developed from the mean spectra of the ears measured with FX10 and FX17 over the entire spectral range of the cameras and over a reduced range of interest.

Camera	Spectral range	Latent variables	Preprocess	Sensitivity (validation)	Specificity (validation)	Error of classification (validation)
FX10	410 – 990 nm	4	Savitzky-Golay 1 st	86.2%	88.5%	12.7%
	900 – 990 nm	2		84.5%	96.2%	9.7%
FX17	965 – 1682 nm	5	derivative	81.9%	98.5%	9.8%
	1055 – 1229 nm	3	(2,7)	85.3%	97.7%	8.5%

¹ Vincke, D., Mercatoris, B., Eylenbosch, D., Baeten, V., Vermeulen, P., 2022. Assessment of kernel presence in winter wheat ears at spikelet scale using near-infrared hyperspectral imaging. *Journal of Cereal Science* 106, 103497. <https://doi.org/10.1016/j.jcs.2022.103497>

Table 2. Performances in validation of the classification models discriminating between parts containing healthy and infected kernels developed on selected pixels from images measured with FX10 and FX17 over the entire spectral range of the cameras.

Camera	Spectral range	Latent variables	Preprocess	Sensitivity (validation)	Specificity (validation)	Error of classification (validation)
FX10	410 – 990 nm	3	Savitzky-Golay 1 st	90.8%	73.5%	17.8%
FX17	965 – 1682 nm	3	derivative (2,7)	96.2%	87.1%	8.3%

2. Discrimination of diseased ear areas at pixel-level

Calibration set: 1000 pixels spectra/class selected from 8 ears (4 healthy and 4 with bunt disease)
Validation set: 1000 pixels spectra/class selected from 4 ears (2 healthy and 2 with bunt disease)
Images test set: 63 ears (36 healthy and 27 with bunt disease)

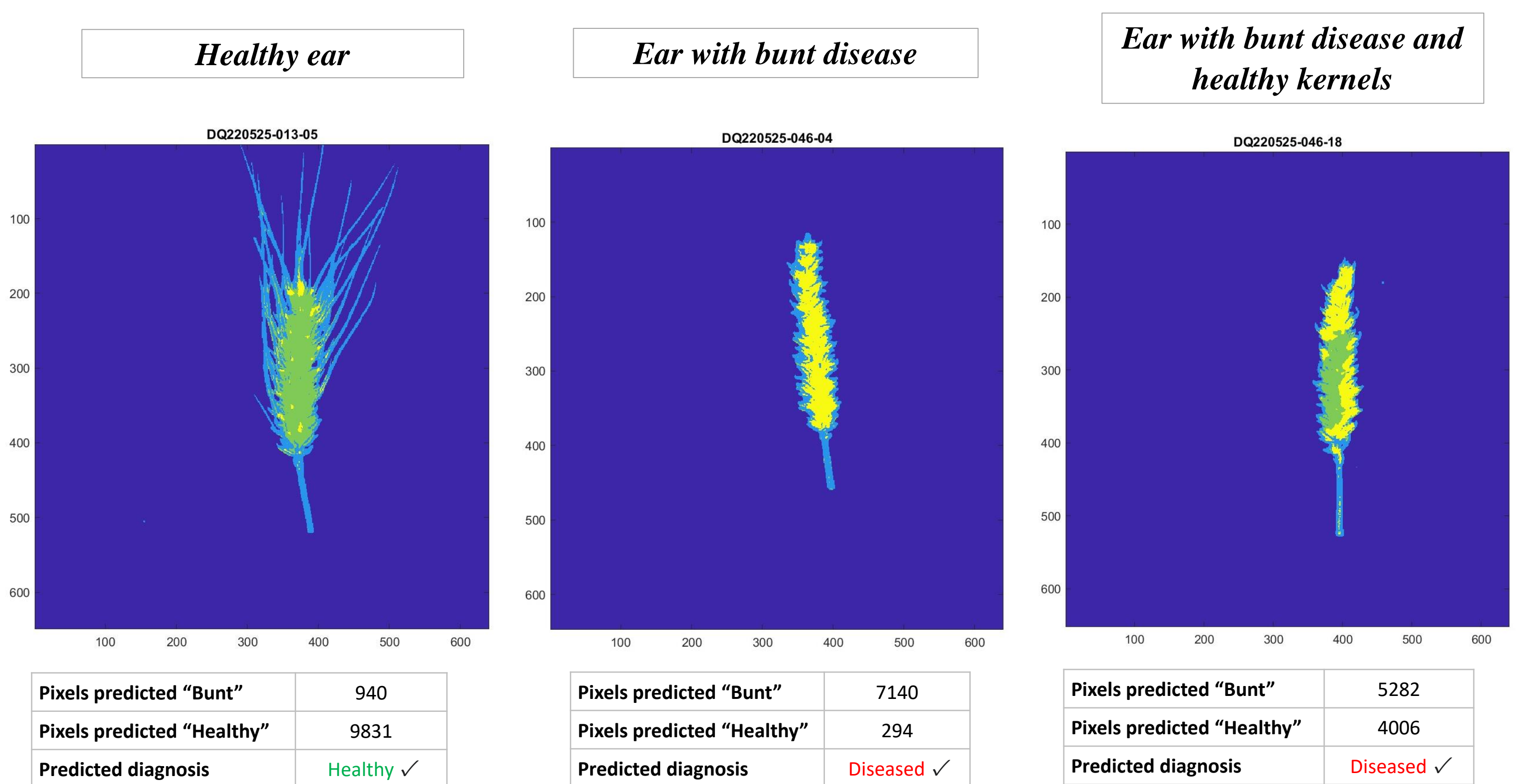


Figure 4. Example of prediction images of wheat ears from the test set after application of the models developed on FX17 at pixel-level.

Conclusions and future prospects

This study shows that there is a spectral difference between healthy and bunt-diseased ears, and therefore that discrimination between the two classes is possible. An assessment of the health status based on the mean spectrum of the ears seems to be sufficient, but a more localized detection of bunt allows the distinction of partially diseased ears. Imaging appears to be a promising method for effectively discriminating between diseased and healthy wheat ears.

NIR HSI will now be investigated as a potential phenotyping tool applied directly in the field (cf. figure 5) to estimate more easily and accurately the extent of bunt disease infestation in a common wheat plot. If results in fields are conclusive, this method could also be used as part of research to evaluate the tolerance of cereal varieties to bunt or the effectiveness of seed protection products on plants before harvest.

The research leading to these results has received funding from Horizon Europe – the Framework Programme for Research and Innovation 2021-2027 (PHENET - Grant agreement 101094587) and from the Wallon Recovery Plan 2022 project 204/2 (ValCerWal).



Figure 5. HSI set-up for field analysis.